ELSEVIER

Journal of Hepatology 44 (2006) 167–175

Journal of Hepatology

www.elsevier.com/locate/jhep

Oral imatinib treatment reduces early fibrogenesis but does not prevent progression in the long term

Markus Neef[1], Monika Ledermann[1], Hans Saegesser[1], Vreni Schneider[1], Nicolas Widmer[2], Laurent Arthur Decosterd[2], Bertrand Rochat[3], Juerg Reichen[1,*]

[1]*Institute of Clinical Pharmacology, University of Berne, Berne, Switzerland*
[2]*Division of Clinical Pharmacology, CHUV University Hospital, Lausanne, Switzerland*
[3]*Quantitative Mass Spectrometry Facility, Centre Hospitalier Universitaire Vaudois, Lausanne CHUV, Switzerland*

***Background/Aims*: Transactivated hepatic stellate cells (HSCs) represent the key source of extra cellular matrix (ECM) in fibrotic liver. Imatinib, a potent inhibitor of the PDGF receptor tyrosine kinase, reduces HSC proliferation and fibrogenesis when treatment is initiated before fibrosis has developed. We tested the antifibrotic potential of imatinib in ongoing liver injury and in established fibrosis.**

***Methods*: BDL-rats were gavage fed with 20 mg/kg/d imatinib either *early* (days 0–21) or *late* (days 22–35) after BDL. Untreated BDL-rats served as controls. ECM and activated HSCs were quantified by morphometry. Tissue activity of MMP-2 was determined by gelatin zymography. mRNA expression of TIMP-1 and procollagen α1(I) were measured by RT-PCR. Liver tissue concentration of imatinib was measured by tandem mass spectrometry.**

***Results*: Early imatinib reduced ECM formation by 30% ($P = 0.0455$) but left numbers of activated HSCs and procollagen I expression unchanged. MMP-2 activity and TIMP-1 expression were reduced by 50%. Late imatinib treatment did not alter histological or molecular markers of fibrogenesis despite high imatinib tissue levels.**

***Conclusions*: The antifibrotic effectiveness of imatinib is limited to the early phase of fibrogenesis. In ongoing liver injury other mediators most likely compensate for the inhibited PDGF effect.**

***Keywords*: Liver cirrhosis; Experimental; Bile duct-ligation; Hepatic stellate cells; Imatinib; Platelet-derived growth factor; Platelet-derived growth factor beta receptor**

1. Introduction

Hepatic stellate cells (HSCs) have been identified as the key source of excess extracellular matrix (ECM) in the fibrotic liver. Following liver injury of any etiology, they become activated from their quiescent state and transform into proliferative, fibrogenic, and contractile myofibroblasts. This process is initiated by paracrine secretion of growth factors and cytokines through neighboring cells whereupon HSCs respond with enhanced growth factor expression and responsiveness [1].

Platelet-derived growth factor (PDGF) is the best characterized and most potent mitogen for cultured HSCs isolated from human or rodent liver. It binds to PDGF receptors (PDGFRs) that belong to the family of receptor tyrosine kinases (RTKs). Transdifferentiation of HSCs coincides with an increased expression of PDGF [2] and a switch in receptor subtype expression from PDGFRα to -β [3]. Expression of PDGF and PDGFRβ is closely correlated with the extent of inflammation in liver tissue of patients with chronic liver diseases [2]. In addition, PDGF is profibrogenic in conditions where inflammation is less evident, such as cholestatic liver injury, where PDGF can also be synthesized by cholangiocytes [4,5]. PDGFRs, like other RTKs, contain an extracellular ligand-binding domain connected to the cytoplasmic domain by a transmembrane helix. Upon ligand binding, PDGFRs dimerize and become autophosphorylated.

Received 19 January 2005; received in revised form 16 June 2005; accepted 24 June 2005; available online 12 July 2005

* Corresponding author. Tel.: +41 31 632 31 91; fax: +41 31 632 49 97.
E-mail address: reichen@ikp.unibe.ch (J. Reichen).

0168-8278/$30.00
doi:10.1016/j.jhep.2005.06.015

Binding of adaptor molecules to phosphotyrosines, in turn, triggers various signaling pathways, including the Ras-ERK and the PI3-Akt pathways resulting eventually in cell proliferation and survival (reviewed in [6]).

Imatinib, formerly known as STI571, is a potent, competitive inhibitor of three tyrosine kinases (PDGFR, Bcr-Abl and c-Kit) [7]. It is in clinical use for the treatment of chronic myeloid leucemia and gastrointestinal stroma tumors. Imatinib produces a dose-dependent inhibition of the proliferation induced by PDGF in cultured rat HSCs. When BDL-rats were treated with imatinib the number of proliferating HSCs 48 h after BDL was reduced by 60% [8]. Similarly, when PDGF was absorbed by a soluble PDGFRβ, fibrogenesis was effectively attenuated for up to 14 days after BDL [9,10]. Recently, the prophylactic potential of imatinib has been underlined by a significant fibrosis reduction during 8 weeks of concomitant stimulation with pig serum [11].

The evaluation of the antifibrotic potential of a given agent requires in vivo models that most closely reproduce human fibrotic liver diseases [12]. Furthermore, prophylaxis (i.e. initiation of treatment before fibrogenesis has started) does not reflect the clinical application of a potential antifibrotic drug. We therefore used the rat model of secondary biliary fibrosis after BDL which is characterized by progressive fibrosis in the absence of inflammation or necrosis to test whether imatinib shows antifibrotic effects when treatment is continued beyond 48 h after BDL and whether it is effective once liver fibrosis is already established.

2. Material and methods

2.1. Animals, bile duct-ligation

Male Wistar rats were kept under a 12 h light-dark cycle with free access to rat chow (Provimi Kliba AG, Kaiseraugst, Switzerland) and water. Induction of biliary fibrosis by bile duct-ligation (BDL) and sham operations were performed under ether anesthesia as previously described [13]. All animals received humane care. Animal experiments were approved by a state-appointed board on animal ethics and were performed according to international guidelines concerning the conduct of animal experimentation.

2.2. Imatinib, D8-imatinib, analytical chemicals

Imatinib and deuterated imatinib (D8-imatinib) were a kind gift by Novartis Pharma (Basel, Switzerland). D8-imatinib was used as internal standard for the determination of imatinib in the liver. All other reagents for the analytical procedure were of HPLC grade.

2.3. Early treatment study: prophylactic imatinib

Twenty BDL-rats were randomly assigned to either treatment with oral imatinib (20 mg/kg/d) for a period of three weeks or to an untreated control group. Imatinib was dissolved in sterile water at a concentration of 40 mg/ml and rats were gavage fed with a gastric tube. Similarly, 10 sham-operated animals were either treated in an analogous manner or not treated. Studies on these animals were performed three weeks after BDL.

2.4. Late treatment study: imatinib in advanced fibrosis

Of an additional 16 BDL-rats five died during the postoperative period. At day 21 after BDL the remaining 11 rats were characterized by the aminopyrine breath test (ABT) [14] and then subdivided into two groups that either received oral imatinib treatment (20 mg/kg/d) for 2 weeks or remained untreated.

2.5. Aminopyrine breath test (ABT)

$^{14}CO_2$ was measured as an index of the rate of hepatic demethylation of di-^{14}C-methylaminoantipyrine (aminopyrine, Amersham Int., Buckinghamshire, UK); it was injected i.p. in a standard dose of 0.5 μCi (0.3 mg) in 0.5 ml saline, and 10-min breath samples were collected for 90 min as previously described [14]. ^{14}C-radioactivity was measured by liquid scintillation counting using a Kontron Betamatic V counter (Kontron Instruments, Montigny le Bretonneux, France). Results are given as the fractional elimination rate constant, ABT-k, which is a sensitive predictor for mortality in BDL-rats [14].

2.6. Haemodynamic measurements and tissue conservation

Haemodynamic measurements were performed under pentobarbital anesthesia. A carotid artery was cannulated with a PE-50 tube (Parsippany, New York, USA). Upon laparotomy another PE-50 tube was introduced into the portal vein via an ileocolic vein. Portal vein pressure and mean arterial pressure (MAP) were monitored by Statham transducers (Braun, Melsungen, Germany). Liver and spleen were removed and weighed. Liver tissue samples were either snap-frozen and stored at −80 °C or stored in RNAlater (Ambion, Huntingdon, UK).

2.7. Gelatin zymography

Proteolytic activity of tissue homogenates was examined by gelatin zymography according to Watanabe et al. [15]. The supernatants of liver homogenate (10 μg of protein) were subjected to 10% SDS-polyacrylamide gel electrophoresis using gels containing 0.3% gelatin. Proteolytic bands of 62 and 65 kDa, corresponding to the active and latent form of matrix metalloproteinase 2 (MMP-2), respectively, were scanned using an Epson Perfection 3200 Photo transillumination scanner (Epson Ltd., Meerbusch, Germany) and densitometric evaluation was performed using AIDA software (Raytek, Sheffield, UK).

2.8. RNA isolation and RT-PCR

Total RNA was isolated from 30 mg of liver tissue using the RNeasy kit (Qiagen, Basel, Switzerland) with DNase treatment (Promega, Wallisellen, Switzerland) followed by reverse transcription with M-MLV reverse transcriptase (Invitrogen, Basel, Switzerland), according to the manufacturers' instructions. Quantitative PCR was carried out on the ABI 7700 Sequence detector (Applied Biosystems, Rotkreuz, Switzerland). Sequences and accession numbers of primers and probes used are summarized in Table 1.

2.9. Histology, immunohistochemistry

Formalin-fixed and paraffin-embedded liver sections (2–3 μm) were used for quantification of fibrosis after chromotrope aniline blue (CAB) staining as described previously [13] (Fig. 1). For α-SMA staining slides were incubated with a mouse anti-SMA (clone 1A4; Sigma-Aldrich, St. Louis, MO) diluted 1:600 in Tris-buffered saline for 60 min. A biotinylated rabbit-anti-mouse secondary antibody, absorbed with rat serum (Dako, Glostrup, Denmark) was applied (1:200, 45 min) and complexed with a streptavidin-conjugated alkaline phosphatase (1:200, 45 min; Dako). Finally, slides were developed in new fuchsin-naphtol AS-BI (Sigma-Aldrich), and counterstained with hematoxylin.

Table 1
Nucleotide sequences of RT-PCR primers and probes

Target mRNA/accession number	Primer/probe	Position	Sequence
Rat GAPDH/NM_017008	Sense primer	1598	5′ CTGCCAAGTATGATGACATCAAGAA 3′
	Antisense primer	1669	5′ AGCCCAGGATGCCCTTTAGT 3′
	Probe	1643	5′ TCGGCCGCCTGCTTCACCA 3′
Rat procollagen α1 chain/ Z78279	Sense primer		5′ AGAGCGGAGAGTACTGGATCGA 3′
	Antisense primer		5′ CTGACCTGTCTCCATGTTGCA 3′
	Probe	3776	5′ CAAGGCTGCAACCTGGATGCCATC 3′
Rat TIMP-1/NM_053819	Sense primer	247	5′ GATTCGACGCTGTGGGAAAT 3′
	Antisense primer	366	5′ GGCCCGCGATGAGAAACT 3′
	Probe	268	5′ CCACAGGTTTCCGGTTCGCCTACAC 3′

Nucleotide sequence of primers and probes used for RT-PCR. Position is defined as the 5′nucleotide of the respective primer or probe related to the source sequence.

2.10. Morphometry

A point counting procedure was carried out using a microscope with a sampling stage and a semiautomatic advancer [14]. In CAB-stained sections, each of 500 points was classified as hepatocyte, bile duct, connective tissue or other. Likewise, α-SMA positive cells in the sinusoidal lining (i.e. surrounded by hepatocytes) were classified as parenchymal HSC and counted. Morphometric results are presented as volume fractions (percentage of specific counts in relation to the total number of counted points).

2.11. Measurement of imatinib concentration in liver tissue

Samples containing 50 mg/ml of wet weight homogenated liver were prepared in phosphate buffer, using a Fast Prep homogenizer (Q-biogene, Basel, Switzerland). For calibration, imatinib was added to untreated livers at final amounts of 0, 2, 10, 20, 50, 100, and 200 ng/mg. D8-imatinib served as internal standard at final amounts of 2 ng/mg. Proteins were precipitated from 100 μl of liver homogenate with 200 μl of acetonitrile and centrifuged (10,000 g, 10 min). The resulting supernatants (5 μl) were injected onto a Waters RP8 Symmetry shield analytical column (2.1 mm ID×30 mm length) (Waters, Milford, MA, USA). Mobile phase consisted of A: 10 mM ammonium acetate +1% acetic acid and B: methanol +1% acetic acid. Gradient was as following: 0 min: 20% of B, 3 min: 80% of B and 6 min: 98% of B. Flow rate was 0.3 ml/min and total run time was 16 min. No carry over was observed. The system (LC–MS/MS) consisted of an Agilent HP1100 binary pump (Agilent Technologies, Palo Alto, USA) coupled to a triple quadrupole mass spectrometer (TSQ Quantum, Thermo Corporation, San Jose, CA, USA). With the electrospray ionization in positive mode, $(M+H)^+$ precursor to product ions of 494–394, 480–394 and 510–410 and 502–394 amu were chosen as transitions for imatinib, *N*-demethyl-imatinib, potential hydroxy or *N*-oxide metabolites and D8-imatinib. Imatinib/D8-imatinib ratios were used for quantitation of imatinib in rat liver homogenates by comparison with the calibration curve (quadratic regression and 1/concentration^2 weighted). Standard deviation of calibrators was <10%.

2.12. Statistics

Groups of treated and untreated rats were compared with the Mann–Whitney-U test for non-parametric comparison of unrelated samples using the Stat-View statistics software (SAS Institute Inc., Cary, NC, USA). Results were considered statistically significant with a $P<0.05$. Results are given as mean±standard deviation (SD). Whiskers, box margins, and the midline of box plots depict the 10th, 25th, 50th, 75th, and 90th percentile of the respective variable.

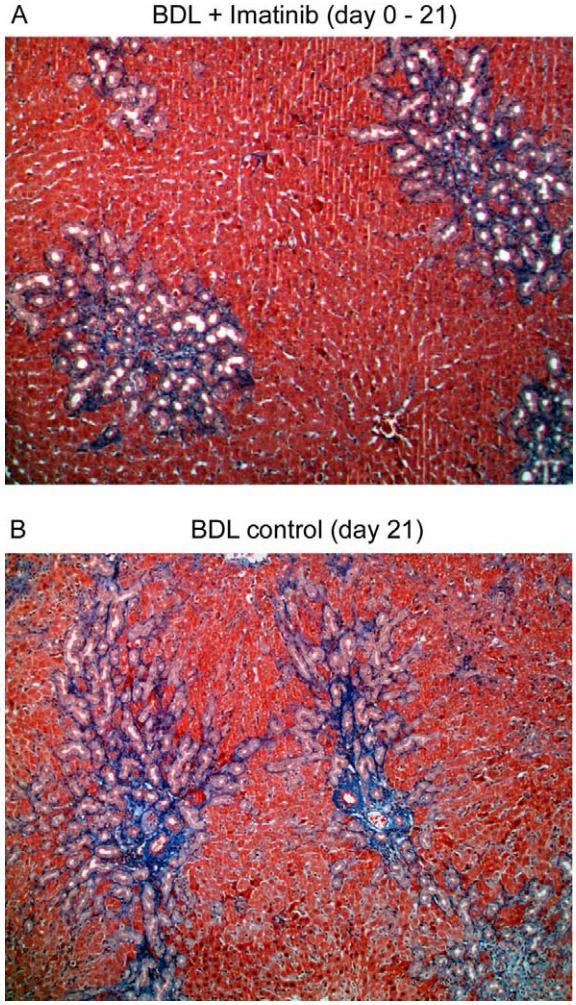

Fig. 1. Liver histology after chromotrope aniline blue staining (blue = extracellular matrix (ECM) proteins; red = hepatocytes, pink = bile duct epithelial cells). (A+B) Following BDL rats were treated with 20 mg/kg/d oral Imatinib for 21 days (BDL+Imatinib, *n* = 8) (A) or left untreated for the same period (BDl control, *n* = 7) (B). Original magnification×100.

3. Results

3.1. Early imatinib treatment

3.1.1. Animal characterization and haemodynamics

Four rats died during the first five days after BDL. Two belonged to the treatment group and two were untreated. No further animals died during the last 2 weeks of the experiment. One imatinib treated rat was found to have a restored bile flow on laparotomy and was excluded from analysis. Three weeks after BDL ABT showed comparably impaired liver function in both treated and untreated rats (Table 2). Liver weight was increased in all BDL-rats compared with sham-operated rats ($P<0.0001$), but lowered by imatinib treatment ($P=0.049$). Body weights were decreased in BDL-rats ($P=0.004$) compared to sham-rats but were not altered in the imatinib treated group. Concomitantly, portal pressure and spleen weights were markedly elevated in BDL-rats compared to sham-operated controls ($P<0.0001$) but were not affected by imatinib treatment. This was accompanied by unchanged MAP or heart rate. Detailed values are given in Table 2.

3.2. Reduced fibrosis in early imatinib treatment

BDL alone over 3 weeks resulted in massive bile duct proliferation and fibrosis. Volume fractions of ECM were increased more than 10-fold compared to sham-operated groups (15.9 ± 5 vs. $1.32\pm0.5\%$, respectively; $P<0.0001$). This increase was significantly prevented by 30% in rats treated with imatinib compared with non-treated BDL-rats ($11.23\pm3.7\%$; $P=0.0455$) (Fig. 2). Abundance of activated (α-SMA positive) HSCs was markedly increased 3 weeks after BDL compared with sham-operated animals (0.6 ± 0.3 vs. $0.04\pm0.08\%$ volume fractions; $P<0.001$). In contrast to the reduction in ECM formation this increase in α-SMA positive HSCs was not affected by imatinib treatment (Fig. 3).

Similarly, procollagen $\alpha1$ mRNA expression was equal in both groups (Fig. 3A). Discrepant results for the histological amount of collagen and procollagen mRNA expression have been reported earlier and have been ascribed to the posttranscriptional regulation of collagen expression as found in cultured HSC [9,16]. In liver fibrosis, characteristic expression patterns of matrix metalloproteinases (MMPs) can be observed that play a role in the degradation of normal liver matrix. Conversely, tissue inhibitors of metalloproteinases (namely TIMP-1) block the antifibrotic activity of other MMPs [17]. We therefore measured tissue activity of MMP-2 by gelatinase zymography and TIMP-1 expression by RT-PCR, respectively, and found a significant 47% reduction in MMP-2 activation, measured as ratio of active vs. latent MMP-2 (0.23 ± 0.13 in imatinib treated vs. 0.37 ± 0.12 in control animals, respectively; $P=0.0389$) (Fig. 4). Likewise, mRNA steady state levels of TIMP-1 were reduced by 50% in treated compared to control rats ($P=0.0169$; Fig. 3B).

3.3. Imatinib in established cirrhosis

3.3.1. Animal characterization and haemodynamics

Serum bilirubin levels were comparably elevated in the group of BDL-rats that received late imatinib treatment (20 mg/kg/d, day 22–35) and in the non-treated control group, indicating complete BDL (data not shown). ABT revealed equally impaired liver function in both groups. Body weights did not differ significantly between the two groups. Liver weights were elevated in both groups. Neither

Table 2
Body and organ weights, hemodynamic characteristics, and liver function

	Sham+early imatinib (day 1–21 post BDL)		BDL+early imatinib (day 1–21 post BDL)		BDL+late imatinib (day 21–35 post BDL)	
	Sham IMA $n=5$	Sham CTR $n=5$	BDL-IMA d 0–21 $n=8$	BDL-CTR d 21 $n=7$	BDL-IMA 22–35 $n=7$	BDL-CTR d 35 $n=4$
Body weight (g)	384.8 ± 6.5	420.6 ± 28.9[a]	347.8 ± 32.7	344.0 ± 34.9	438.9 ± 49.4	453.0 ± 36.9
Liver weight (g/kg BW)	15.0 ± 1.9	17.3 ± 1.2[b]	80.1 ± 5.6[c]	90.3 ± 8.9	81.5 ± 13.8	82.6 ± 4.7
Spleen weight (g/kg BW)	2.86 ± 0.73[a]	1.97 ± 0.16[b]	6.5 ± 1.6	7.1 ± 1.4	4.8 ± 0.8	4.8 ± 0.8
MAP (mm Hg)	107.5 ± 21.5	94.8 ± 17.6	90.1 ± 19.2	99.3 ± 11.3	85.9 ± 14.4	102.3 ± 9.7
Heart rate (min^{-1})	365.0 ± 21.8	370.0 ± 22.8	321.4 ± 24.7	345.7 ± 26.1	301.4 ± 11.3	325.0 ± 15.0
Portal pressure (mm Hg)	9.0 ± 0.7	8.2 ± 1.2[b]	15.0 ± 2.6	14.7 ± 1.48	13.7 ± 3.2	12.0 ± 2.4
End of treatment ABT-k ($-h^{-1}$)	n.d	n.d.	0.83 ± 0.22	0.68 ± 0.18	0.18 ± 0.1	0.24 ± 0.1

[a] $P<0.001$ sham vs. BDL+early imatinib.
[b] $P<0.0001$ sham vs. BDL+early imatinib.
[c] $P<0.05$ BDL IMA d 0–21 vs. BDL CTR d 21.

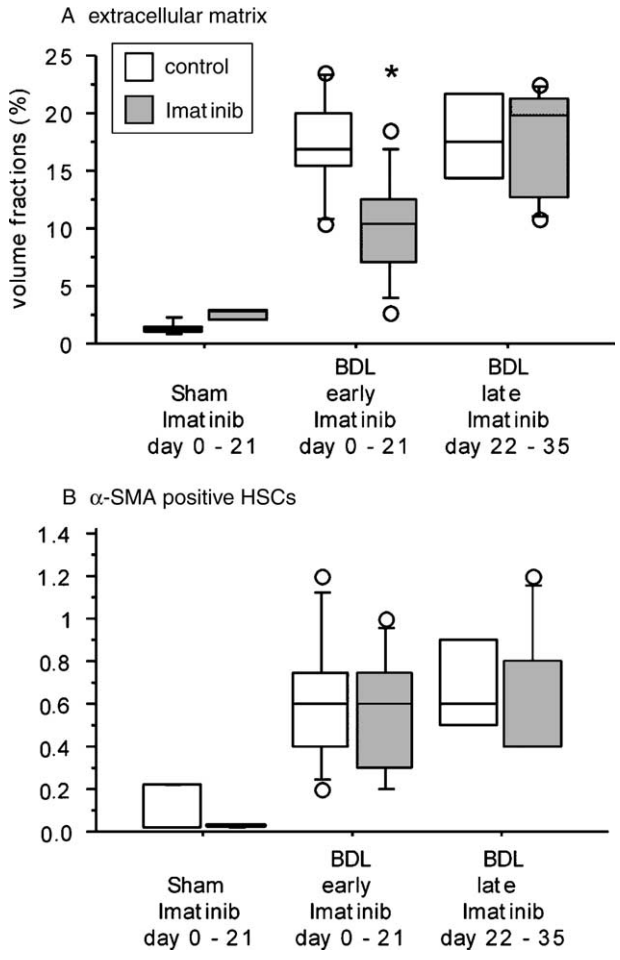

Fig. 2. Effects of imatinib on extracellular matrix (ECM) formation (A) and α-SMA expression (B). Early imatinib treatment (20 mg/kg/d p.o.; day 0–21) was given to sham-operated and BDL-rats. Late imatinib treatment (day 22–35 after BDL) was given to BDL-rats only. Untreated sham-operated or BDL-rats served as controls (sham imatinib: $n=5$, control $n=5$; BDL early imatinib: $n=8$, control $n=7$; BDL late imatinib: $n=7$, control $n=4$). Morphometric analysis was carried out after chromotrope aniline blue-staining for ECM components and α-SMA immunohistochemistry, respectively. Five hundred randomly chosen points were classified as positive or negative for ECM or α-SMA staining, respectively. Results are given as volume fractions (i.e. the percentage of specific counts in relation to the total number of counted points). * Prophylactic imatinib treatment inhibited ECM production ($P=0.0455$) but did not affect volume fractions of α-SMA positive cells.

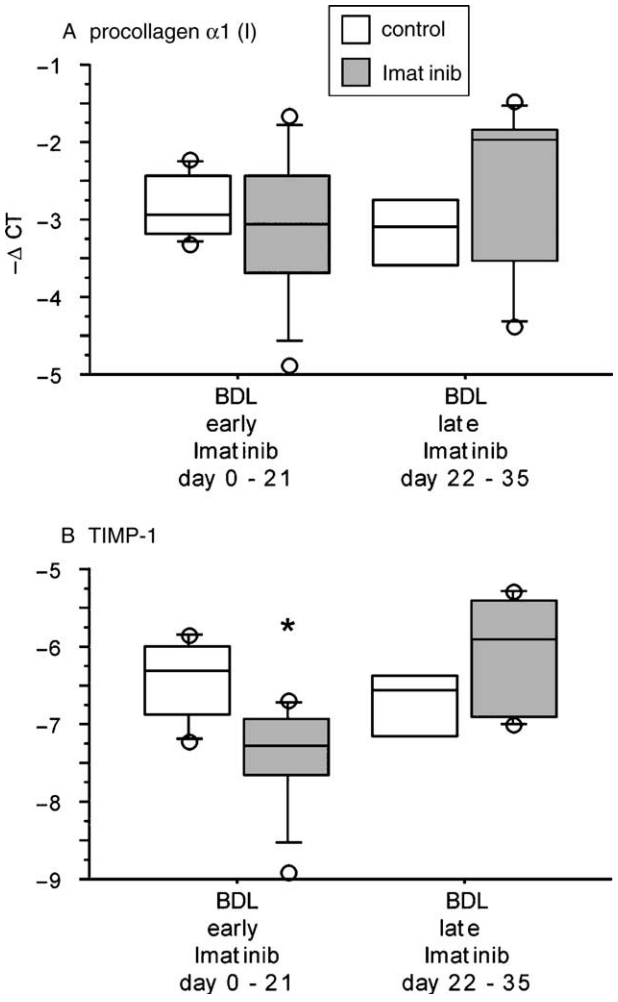

Fig. 3. Effects of imatinib treatment on total liver procollagen α1 (I) and TIMP-1 mRNA expression. Rats received imatinib treatment (20 mg/kg/d p.o.) either early (days 0–21) or late (days 22–35) after BDL or were left untreated for the same period as control (BDL early Imatinib: $n=8$, control $n=7$; BDL late Imatinib: $n=7$, control $n=4$). Results of quantitative real time-PCRs are given as $-\Delta Ct$ values, lower $-\Delta Ct$ values denote lower mRNA levels and vice versa. * Prophylactic imatinib reduced TIMP-1 mRNA expression ($P=0.017$) but did not alter procollagen α1 mRNA expression.

liver nor spleen weights differed between the two groups. Haemodynamic measurement did not show significant differences between the two groups (Table 2).

3.3.2. No detectable antifibrotic effect of imatinib in established cirrhosis

In contrast to the early treatment experiment, there were no significant differences in ECM formation or HSC activation, measured by morphometric evaluation of CAB-staining or α-SMA Immunohistochemistry, respectively (Fig. 2). Similarly, procollagen α1 and TIMP-1 mRNA expression as well as MMP-2 activity showed no significant differences between the treated and non-treated group (Figs. 3 and 4).

3.3.3. High imatinib concentrations in liver tissue of treated animals

Imatinib concentrations in liver homogenates were significantly higher in late treated compared with early treated livers (14.0 ± 4.3 vs. 7.0 ± 3.4 ng/mg liver tissue; $P=0.003$) (Fig. 5A) whereby imatinib concentrations correlated inversely with liver function as measured by ABT ($r^2=0.67$; $P=0.001$; Fig. 5B). Imatinib metabolites *N*-demethyl-imatinib and hydroxy or *N*-oxide metabolites were detectable in all treated animals demonstrating hepatic metabolism of imatinib via the cytochrome P-450 system (Fig. 6).

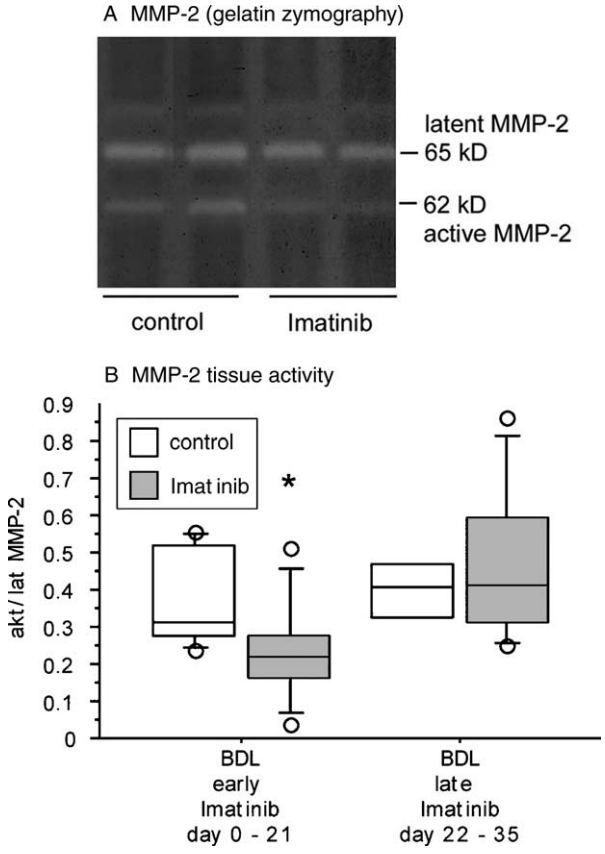

Fig. 4. Effect of imatinib treatment on liver tissue activity of MMP-2 collagenase measured by gelatin zymography. Rats received imatinib treatment (20 mg/kg/d p.o.) either early (days 0–21) or late (days 22–35) after BDL or were left untreated for the same period as controls (BDL early Imatinib: $n=8$, control $n=7$; BDL late Imatinib: $n=7$, control $n=4$). (A) 20 μg of each liver protein sample from control and Imatinib treated animals were analyzed by gelatin zymography. (B) Quantitative analysis by densitometry showed a significant reduction in MMP-2 tissue activity after 3 weeks of early Imatinib treatment *($P=0.039$) but not after late Imatinib treatment.

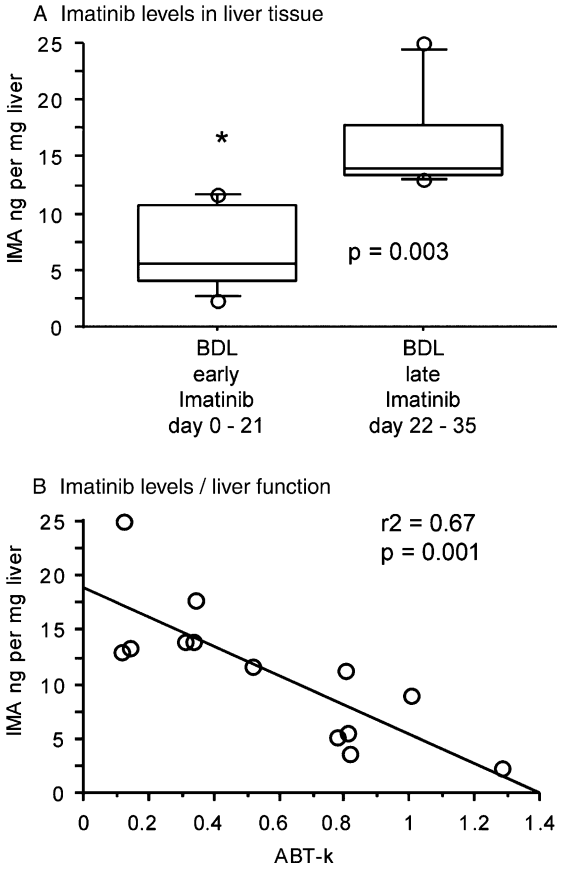

Fig. 5. (A+B) Imatinib tissue concentrations were measured by tandem mass spectrometry, liver function was measured by aminopyrine breath test (ABT) in livers of BDL-rats that had been treated with imatinib (20 mg/kg/d) either early (day 0–21, $n=8$) or late (day 22–35, $n=7$) after BDL. (A) * Imatinib levels were significantly higher ($P=0.003$) in late treated animals and (B) correlated inversely with liver function ($r^2=0.67$; $P=0.001$).

4. Discussion

Abundant evidence has confirmed the involvement of PDGF and its respective receptors in the activation process of HSCs. Therefore PDGF signaling has repeatedly been postulated as an attractive therapeutic target [8,9,18,19]. To our knowledge, the present study is the first to investigate the therapeutic potential of imatinib, a potent inhibitor of the PDGF-R tyrosine kinase, for a period longer than 48 h after BDL or in established fibrosis.

We found that prophylactic imatinib markedly reduced fibrosis up to three weeks after BDL, associated with a reduction in MMP-2 activity and expression levels of TIMP-1. In contrast, the amount of activated HSCs or portal pressure were not affected. When imatinib was initiated in a state of advanced fibrosis, it neither reduced numbers of activated HSCs nor did it inhibit ECM production. Likewise, the effects on molecular markers of fibrogenesis, that had been observed in the early treatment experiment, were no longer evident.

At first, this difference in antifibrotic response between early and late treatment raised the question whether the drug had effectively reached its cellular targets in fibrotic livers. However, high imatinib tissue concentrations were found in both early and late treated livers, suggesting that the lack of an antifibrotic effect was not due to reduced drug availability in liver tissue. An inverse correlation of liver function and imatinib levels indicated that drug metabolism via the cytochrome P450 system was impaired in fibrotic livers resulting to the contrary in higher drug-on-target levels in advanced fibrosis.

The antifibrotic effect that we found after prophylactic imatinib treatment confirms and expands previous observations that showed a similar reduction of fibrosis when livers were examined 48 h after BDL [8]. Likewise, absorption of free PDGF-BB with a soluble PDGF-Rβ prompted a significant decrease in ECM deposition fourteen days after BDL [9]. These results were mainly ascribed to an

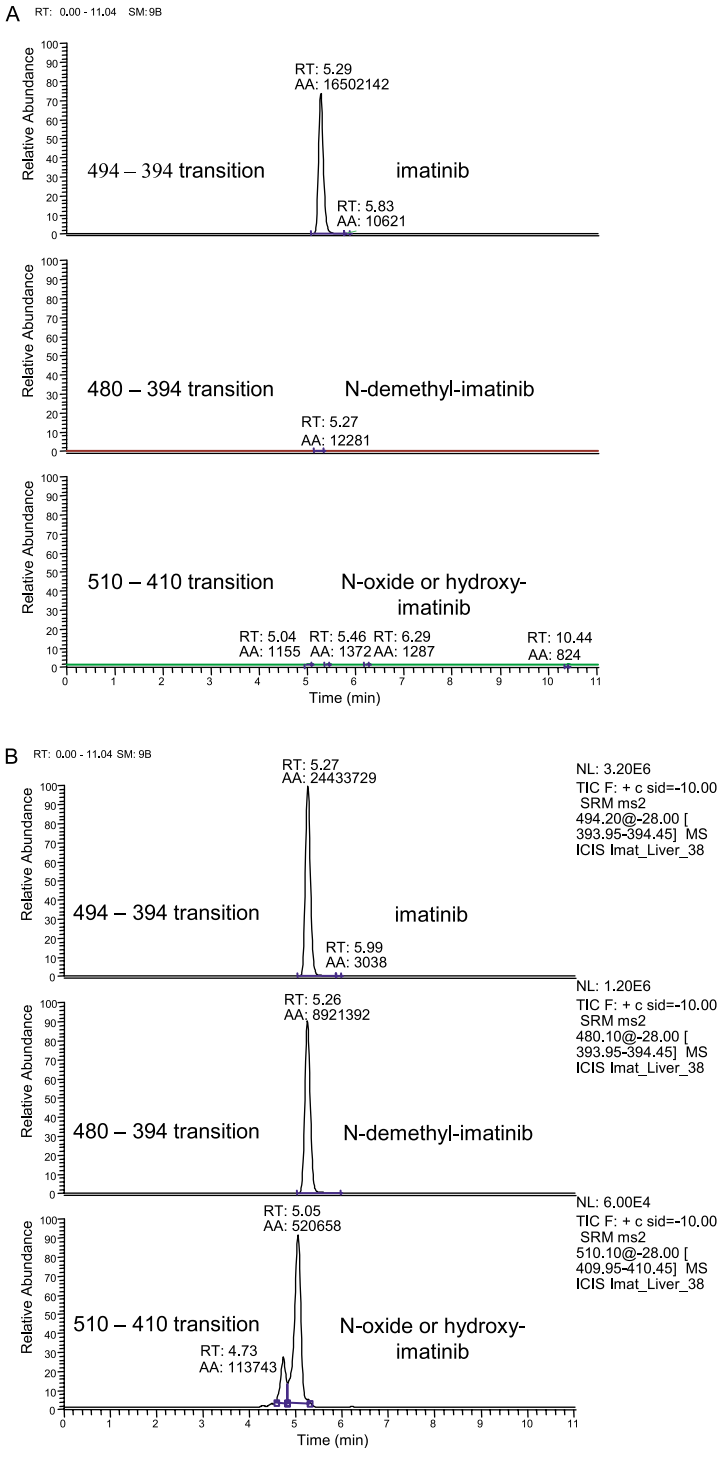

Fig. 6. LC–MS/MS chromatograms of extracts of 2 rat liver homogenates. Three transitions (masses of precursor to product ions) were applied and correspond to imatinib, *N*-demethyl-imatinib and *N*-oxide or hydroxy-imatinib. (A) An untreated liver homogenate spiked with imatinib at 20 ng/mg of wet weight. (B) Homogenate from a rat treated with 20 mg/kg/d imatinib quantified at 25 ng/mg of wet weight. Same scales (abundance against time) are displayed for both chromatograms. Retention times were between 5.0 and 5.3 min for all compounds.

antiproliferative effect on HSCs rather than inhibited synthesis of fibrogenic markers per se [9]. In agreement with this notion the above cited studies showed a reduction of α-SMA immunostaining that was more pronounced than the reduction of ECM deposition.

At first glance this is in contradiction to our early treatment study that failed to demonstrate a reduction in α-SMA positive HSCs. The important difference lies in the time point of observation: we clearly show that HSC proliferation was not abrogated under imatinib treatment

in the long term. Moreover, the increase in activated HSCs was paralleled by elevated portal pressures despite lesser amount of fibrosis in the early treatment study. This strongly suggests that other mediators may compensate for the inhibited PDGF and that PDGF is not exclusively essential for HSC proliferation. Thus, assuming that HSC proliferation is delayed but not abolished under imatinib, it is conceivable that the production of ECM components also lags behind. This hypothesis may prove valid also with regard to a recent study that showed a massive inhibition of α-SMA expression after 8 weeks of prophylactic imatinib concomitant with pig-serum treatment [11]. In contrast to BDL, this imposes on the liver a much weaker fibrogenic stimulus (e.g. pig serum-treatment resulted in 1.5% fibrotic areas after 8 weeks vs. 16% after 5 weeks BDL), which is generated by higher degrees of parenchymal necrosis. Presumably, this fundamentally different pathogenesis gives rise to a pattern of mediators that renders fibrosis progression more susceptible to PDGF-inhibition. However, it does not mirror the common human chronic liver disease [12].

The results of our late treatment study are in accordance with earlier observations suggesting that regression of fibrosis requires apoptosis of HSCs rather than antiproliferation [20,21] and that activation and survival (anti-apoptosis) are under the control of different cytokines [22]. PDGF and insulin-like growth factor-I (IGF-I) provide examples of this effect. While both cytokines are equipotent in the activation of the Ras/ERK and the PI3-K pathway at least at early time points after stimulation, IGF-1 induces only one-fifth of the increase in DNA synthesis [23] but in turn activates the c-Akt pathway and thereby regulates cell survival rather than proliferation [24].

Our study supports the concept that alternative cytokines and/or pathways can compensate for the mitogenic effect of PDGF in ongoing liver injury. Furthermore, it underlines the point that survival of fibrogenic cells after their activation is independent of PDGF. Therefore, as proposed by others, antifibrotic treatment needs to be targeted against more than one single signaling system due to their overlapping modes of action. Future investigations in our laboratory will evaluate this hypothesis.

In conclusion, we provided evidence that imatinib alone is not effective in inhibiting HSC proliferation in ongoing cholestatic liver injury in the long term and becomes ineffective when fibrosis has already developed.

Acknowledgements

This study was supported by a grant from the Swiss National Foundation for Scientific Research (3200B0-105601/1) to JR.

References

[1] Friedman SL. The hepatic stellate cell. In: Berk PD, editor. Semin Liver Dis. New York: Thieme; 2001. p. 307–452.
[2] Pinzani M, Milani S, Herbst H, DeFranco R, Grappone C, Gentilini A, et al. Expression of platelet-derived growth factor and its receptors in normal human liver and during active hepatic fibrogenesis. Am J Pathol 1996;148:785–800.
[3] Wong L, Yamasaki G, Johnson RJ, Friedman SL. Induction of beta-platelet-derived growth factor receptor in rat hepatic lipocytes during cellular activation in vivo and in culture. J Clin Invest 1994;94: 1563–1569.
[4] Grappone C, Pinzani M, Parola M, Pellegrini G, Caligiuri A, DeFranco R, et al. Expression of platelet-derived growth factor in newly formed cholangiocytes during experimental biliary fibrosis in rats. J Hepatol 1999;31:100–109.
[5] Kinnman N, Hultcrantz R, Barbu V, Rey C, Wendum D, Poupon R, et al. PDGF-mediated chemoattraction of hepatic stellate cells by bile duct segments in cholestatic liver injury. Lab Invest 2000;80: 697–707.
[6] Heldin CH, Ostman A, Ronnstrand L. Signal transduction via platelet-derived growth factor receptors. Biochim Biophys Acta 1998;1378: F79–F113.
[7] Buchdunger E, Cioffi LC, Law D, Stover S, Ohno-Jones BJ, et al. Abl protein-tyrosine kinase inhibitor STI571 inhibits in vitro signal transduction mediated by c-kit and platelet-derived growth factor receptors. J Pharmacol Exp Ther 2000;295:139–145.
[8] Kinnman N, Goria O, Wendum D, Gendron MC, Rey C, Poupon R, et al. Hepatic stellate cell proliferation is an early platelet-derived growth factor-mediated cellular event in rat cholestatic liver injury. Lab Invest 2001;81:1709–1716.
[9] Borkham-Kamphorst E, Herrmann J, Stoll D, Treptau J, Gressner AM, Weiskirchen R. Dominant-negative soluble PDGF-beta receptor inhibits hepatic stellate cell activation and attenuates liver fibrosis. Lab Invest 2004;84:766–777.
[10] Borkham-Kamphorst E, Stoll D, Gressner AM, Weiskirchen R. Inhibitory effect of soluble PDGF-beta receptor in culture-activated hepatic stellate cells. Biochem Biophys Res Commun 2004;317: 451–462.
[11] Yoshiji H, Noguchi R, Kuriyama S, Ikenaka Y, Yoshii J, Yanase K, et al. Imatinib mesylate (STI571: Gleevec) attenuates liver fibrosis development in rats. Am J Physiol Gastrointest Liver Physiol 2004; 23:23.
[12] Schuppan D, Strobel D, Hahn EG. Hepatic fibrosis—therapeutic strategies. Digestion 1998;59:385–390.
[13] Biecker E, De Gottardi A, Neef M, Unternahrer M, Schneider V, Ledermann M, et al. Long-term treatment of bile duct ligated rats with (sirolimus) rapamycin significantly attenuates liver fibrosis: Analysis of the underlying mechanisms. J Pharmacol Exp Ther 2005;15:15.
[14] Gross Jr JB, Reichen J, Zeltner TB, Zimmermann A. The evolution of changes in quantitative liver function tests in a rat model of biliary cirrhosis: correlation with morphometric measurement of hepatocyte mass. Hepatology 1987;7:457–463.
[15] Watanabe T, Niioka M, Ishikawa A, Hozawa S, Arai M, Maruyama K, et al. Dynamic change of cells expressing MMP-2 mRNA and MT1-MMP mRNA in the recovery from liver fibrosis in the rat. J Hepatol 2001;35:465–473.
[16] Yata Y, Gotwals P, Koteliansky V, Rockey DC. Dose-dependent inhibition of hepatic fibrosis in mice by a TGF-beta soluble receptor: implications for antifibrotic therapy. Hepatology 2002;35: 1022–1030.
[17] Benyon RC, Arthur JM. Extracellular matrix degradation and the role of hepatic stellate cells. Semin Liver Dis 2001;21: 373–384.

[18] Pinzani M, Gentilini A, Caligiuri A, De Franco R, Pellegrini G, Milani S, et al. Transforming growth factor-beta 1 regulates platelet-derived growth factor receptor beta subunit in human liver fat-storing cells. Hepatology 1995;21:232–239.

[19] Iwamoto H, Nakamuta M, Tada S, Sugimoto R, Enjoji M, Nawata H. Platelet-derived growth factor receptor tyrosine kinase inhibitor AG1295 attenuates rat hepatic stellate cell growth. J Lab Clin Med 2000;135:406–412.

[20] Iredale JP, Benyon RC, Pickering J, McCullen M, Northrop M, Pawley S, et al. Mechanisms of spontaneous resolution of rat liver fibrosis. Hepatic stellate cell apoptosis and reduced hepatic expression of metalloproteinase inhibitors. J Clin Invest 1998; 102:538–549.

[21] Saile B, Knittel T, Matthes N, Schott P, Ramadori G. CD95/CD95L-mediated apoptosis of the hepatic stellate cell. A mechanism terminating uncontrolled hepatic stellate cell proliferation during hepatic tissue repair. Am J Pathol 1997;151:1265–1272.

[22] Pinzani M, Marra F. Cytokine receptors and signaling in hepatic stellate cells. Semin Liver Dis 2001;21:397–416.

[23] Gentilini A, Marra F, Gentilini P, Pinzani M. Phosphatidylinositol-3 kinase and extracellular signal-regulated kinase mediate the chemotactic and mitogenic effects of insulin-like growth factor-I in human hepatic stellate cells. J Hepatol 2000;32:227–234.

[24] Gentilini A, Romanelli RG, Marra F, Gentilini P, Pinzani M. IGF-I is a survival factor for human hepatic stellate cells (HSC): involvement of PI 3-K and c-Akt (Abstract). J Hepatol 2001;34(Suppl. 1):7.